MOLECULAR AND CELLULAR BIOLOGY, Nov. 2005, p. 9920–9935 Vol. 25, No. 22
0270-7306/05/$08.00+0 doi:10.1128/MCB.25.22.9920–9935.2005

CRMP-2 Is Involved in Kinesin-1-Dependent Transport of the Sra-1/WAVE1 Complex and Axon Formation†

Yoji Kawano,[1,2] Takeshi Yoshimura,[1] Daisuke Tsuboi,[1] Saeko Kawabata,[1] Takako Kaneko-Kawano,[2] Hiromichi Shirataki,[2] Tadaomi Takenawa,[3] and Kozo Kaibuchi[1]*

Department of Cell Pharmacology, Graduate School of Medicine, Nagoya University, 65 Tsurumai, Showa-ku, Nagoya, Aichi 466-8550,[1] Division of Molecular and Cell Biology, Institute for Medical Science, Dokkyo University School of Medicine, 880 Kitakobayashi, Mibu-machi, Tochigi 321-0293,[2] and Department of Biochemistry, Institute of Medical Science, University of Tokyo, 4-6-1 Shirokanedai, Minato-ku, Tokyo 108,[3] Japan

Received 22 January 2005/Returned for modification 5 April 2005/Accepted 6 September 2005

A neuron has two types of highly polarized cell processes, the single axon and multiple dendrites. One of the fundamental questions of neurobiology is how neurons acquire such specific and polarized morphologies. During neuronal development, various actin-binding proteins regulate dynamics of actin cytoskeleton in the growth cones of developing axons. The regulation of actin cytoskeleton in the growth cones is thought to be involved in axon outgrowth and axon-dendrite specification. However, it is largely unknown which actin-binding proteins are involved in axon-dendrite specification and how they are transported into the developing axons. We have previously reported that collapsin response mediator protein 2 (CRMP-2) plays a critical role in axon outgrowth and axon-dendrite specification (N. Inagaki, K. Chihara, N. Arimura, C. Menager, Y. Kawano, N. Matsuo, T. Nishimura, M. Amano, and K. Kaibuchi, Nat. Neurosci. 4:781-782, 2001). Here, we found that CRMP-2 interacted with the specifically Rac1-associated protein 1 (Sra-1)/WASP family verprolin-homologous protein 1 (WAVE1) complex, which is a regulator of actin cytoskeleton. The knockdown of Sra-1 and WAVE1 by RNA interference canceled CRMP-2–induced axon outgrowth and multiple-axon formation in cultured hippocampal neurons. We also found that CRMP-2 interacted with the light chain of kinesin-1 and linked kinesin-1 to the Sra-1/WAVE1 complex. The knockdown of CRMP-2 and kinesin-1 delocalized Sra-1 and WAVE1 from the growth cones of axons. These results suggest that CRMP-2 transports the Sra-1/WAVE1 complex to axons in a kinesin-1-dependent manner and thereby regulates axon outgrowth and formation.

A neuron has two types of highly polarized cell processes, the single axon and multiple dendrites, both of which differentiate from common immature neurites. The specification of an axon is thought to depend on its length relative to the other immature neurites, which are also called minor processes (4, 11). Elongation of one of the minor processes is necessary for axon specification. The difference of dynamics of the actin cytoskeleton in the growth cones between the future axons and dendrites appears to determine axon outgrowth and axon-dendrite specification (5). Accumulating evidence indicates that small GTPase Rac and its effectors, such as WAVE/Scars and Sra-1, are involved in axon formation in *Drosophila melanogaster* (35, 45, 61). WAVEs have a verprolin homology (V) domain, a cofilin homology (C) domain, and an acidic (A) region at the C terminus (53). The V domain is a G-actin-binding site, and the CA domain binds to the Arp2/3 complex. WAVEs form the complex with Sra-1 (the Sra-1/WAVE complex) and activate the Arp2/3 complex, leading to rapid actin polymerization. The Sra-1/WAVE complex is known to be involved in lamellipodia formation downstream of Rac in fibroblasts (14, 49). However, the functions of the Sra-1/WAVE complex in mammalian neurons are largely unknown.

Axonal proteins are thought to be transported by microtubule-dependent motor proteins, such as kinesin. Kinesins are a family of motor proteins that use the energy of ATP hydrolysis to move cargo along microtubules (22, 27). The kinesin superfamily consists of 14 kinesin families (32). Among these, the most information is available for kinesin-1 (conventional kinesin or KIF5/KLC) in nerve tissue. Kinesin-1 is a tetramer of two kinesin heavy chains (KHCs or KIF5s) and two kinesin light chains (KLCs) (6, 26, 56). Kinesin-1 transports several cargo proteins to axons (15) and thereby is engaged in axonogenesis (2, 54).

CRMP/TOAD-64/Ulip2/DRP-2 is a member of at least five isoforms (CRMP-1 to CRMP-4 and CRAM), and its expression is up-regulated during development (9, 17, 18, 24, 39). We have previously shown that CRMP-2 is enriched in the distal part of growing axons of cultured hippocampal neurons and that the overexpression of CRMP-2 induces the formation of multiple axons (23). The expression of a dominant-negative form of CRMP-2 or the knockdown of CRMP-2 suppresses axon formation (23, 41, 60). CRMP-2 appears to be crucial for axon outgrowth and axon-dendrite specification. Glycogen synthase kinase 3β phosphorylates and inactivates CRMP-2 downstream of the phosphatidylinositol 3-kinase-Akt pathway, thereby regulating neuronal polarity (60). CRMP-2 interacts with tubulin, Numb, chimaerin, and phospholipase D (8, 16, 33, 41). The interaction of CRMP-2 with tubulin dimers pro-

* Corresponding author. Mailing address: Department of Cell Pharmacology, Graduate School of Medicine, Nagoya University, 65 Tsurumai, Showa-ku, Nagoya, Aichi 466-8550, Japan. Phone: 81-52-744-2074. Fax: 81-52-744-2083. E-mail: kaibuchi@med.nagoya-u.ac.jp.

† Supplemental material for this article may be found at http://mcb.asm.org/.

motes microtubule assembly for axon outgrowth (16). CRMP-2 is also involved in the polarized Numb-mediated endocytosis of the neuronal adhesion molecule L1 at the growth cones (41). We have recently found that CRMP-2 directly binds to KLC of kinesin-1 (30). CRMP-2 appears to be transported by kinesin-1 and to accumulate at the distal part of growing axons. However, it remains unknown whether CRMP-2 regulates axon formation through the reorganization of the actin cytoskeleton and, if so, how it is regulated by CRMP-2.

Here we found that CRMP-2 interacted with the Sra-1/WAVE1 complex and that CRMP-2 was involved in the kinesin-1-dependent transport of the Sra-1/WAVE1 complex to the growth cones of axons. CRMP-2 appears to regulate axon outgrowth and formation through the transport of the Sra-1/WAVE1 complex to the growth cones of developing axons.

MATERIALS AND METHODS

cDNAs encoding human CRMP-2, Sra-1, and WAVE1 were obtained as described previously (1, 31, 38). pCAGGS vector was provided by M. Nakafuku (Cincinnati Children's Hospital Medical Center, Cincinnati, OH). Anti–CRMP-2 monoclonal antibody (C4G) was provided by Y. Ihara (Tokyo University, Tokyo, Japan) (20). Anti-Numb polyclonal antibody (92425) was provided by H. Okano (Keio University, Tokyo, Japan). Anti–CRMP-2 polyclonal, anti-Sra-1, and anti-WAVE1 polyclonal antibodies were obtained as described previously (23, 31, 38). Anti-WAVE1 monoclonal (Transduction Laboratories, Lexington, KY), anti-myc polyclonal, anti-Rho GDI (A-14, A-20; Santa Cruz Biotechnology, Inc., Santa Cruz, CA), antiactin, and anti-Tau-1 monoclonal antibodies (Chemicon, Temecula, CA) as well as anti-myc monoclonal (9E10) antibody and tetramethyl rhodamine isocyanate-phalloidin (Sigma Chemical Co., St. Louis, MO) were purchased. A rabbit polyclonal antibody against KLC 1 was generated by using glutathione *S*-transferase (GST)–KLC 1 wild type (WT) as an antigen (30). Other materials and chemicals were obtained from commercial sources.

Plasmid constructs. pCAGGS-HA and myc-CRMP-2 WT, pGEX-CRMP-2 deletion mutants, and pEF BOS-myc-Sra-1 and WAVE1 dominant negative (DN) were obtained as described previously (16, 31, 38). The cDNA of CRMP-2, in which Asn replaced Asp at position 71, was generated with a site-directed mutagenesis kit (Stratagene, La Jolla, CA). RNA interference (RNAi)-resistant CRMP-2 and Sra-1 (RrCRMP-2 and RrSra-1) were generated with a site-directed mutagenesis kit by using primer GATCACGGGGTAAATAGTTTCCT AGTGTACATGGCTTTCA for CRMP-2 and GCTGAAGAACATGAAATG CAGTGTGAAGAACG for Sra-1. CRMP-2 D71N, KIF5A headless (HL) (amino acids [aa] 402 to 1028), KLC tetratropeptide repeats (TPR) (aa 375 to 542), Sra-1 1-400, Sra-1 401-800, and Sra-1 801-1253 were subcloned into pCR-TOPOII or pENTR vector (Invitrogen) and then transferred into pB-GEX-kk-1 (rearranged vector from pGEX), pGEX (Amersham Pharmacia Biotech, Buckinghamshire, United Kingdom), pDEST15 (Invitrogen), or pCAGGS-myc vector. To obtain recombinant full-length Myc-Sra-1 by the baculovirus expression system, Sra-1 WT was subcloned into pAcYM-1 vector.

Protein purification. GST fusion proteins were purified according to the manufacturer's protocol. Myc–Sra-1 WT was produced in *Spodoptera frugiperda* cells in a baculovirus system and purified as described previously (29, 36).

Affinity column chromatography. Six nanomoles of GST, CRMP-2 WT-GST, and CRMP-2 D71N-GST was separately immobilized onto glutathione-Sepharose 4B (Amersham Pharmacia Biotech). Porcine brain extract was loaded onto immobilized beads. The beads were then washed with buffer A (20 mM Tris-HCl [pH 7.5], 1 mM EDTA, and 1 mM dithiothreitol) that contained 150 mM NaCl, and the bound proteins were eluted with buffer A that contained 10 mM glutathione.

In vitro binding assay. Five-hundred picomoles of GST proteins was separately immobilized onto glutathione-Sepharose 4B. The immobilized beads were incubated with Myc–Sra-1 (0.5 μM) or porcine brain extract for 1 h at 4°C. The beads were then washed six times with buffer A that contained 150 mM NaCl, and the bound proteins were eluted with buffer A that contained 10 mM glutathione.

Immunoprecipitation assay. Porcine brain was extracted by the addition of lysis buffer (20 mM Tris-HCl, 50 mM NaCl, 1 mM EDTA, and 0.1% NP-40 [pH 7.5]) and then clarified by centrifugation at 100,000 × *g* for 20 min at 4°C. The soluble supernatants were incubated with rabbit immunoglobulin G (IgG) or the indicated antibodies for 2 h at 4°C. The immunocomplexes were then precipitated with protein A-Sepharose 4B (Amersham Pharmacia Biotech). The obtained elutes were divided by sodium dodecyl sulfate-polyacrylamide gel electrophoresis (SDS-PAGE).

Cell culture. Culture of hippocampal neurons prepared from embryonic day 18 (E18) rat embryos using papain was performed as described previously (23). Neurons were seeded on coverslips or dishes with poly-D-lysine (PDL; Sigma) and laminin (Iwaki, Tokyo, Japan) for day in vitro 3 (DIV3) or PDL only for DIV6 in Neurobasal medium (Invitrogen) supplemented with B-27 supplement (Invitrogen) and 1 mM glutamine. CRMP-2 has the ability to convert minor processes and preexisting dendrites to axons (23). To visualize secondary axons, neurons at DIV6 are better than those at DIV3, because the secondary axons appear later. In DIV3, the overexpression of CRMP-2 slightly increased the number of cells bearing multiple axon-like neurites, whereas the stronger effect of CRMP-2 was observed in DIV6 (23). A normal neuron has one axon and some dendrites on PDL alone or PDL and laminin. We cultured neurons on glasses coated with PDL and laminin to measure the neurite length at DIV3, because laminin enhances neurite elongation. We cultured neurons on glasses coated with PDL alone to visualize secondary axons, because we were afraid that primary axons that are too elongated sometimes mask the secondary axons on glasses coated with PDL and laminin.

HEK293 cells were cultured at 37°C in an air–5% CO_2 atmosphere at constant humidity. Transfections were carried out using Lipofectamine reagent (Invitrogen).

siRNA preparation and transfection. A 21-oligonucleotide siRNA duplex was designed as recommended by the manufacturer and synthesized by Japan Bio Service (Saitama, Japan) to target the human, mouse, and rat Sra-1 sequence 5′-GAACAUGAAGUGCAGUGUG-3′, rat WAVE1 sequence 5′-CUGAGUA GCCUAAGUAAGG-3′, rat KLC-1 5′-ATACGACGACGACATCTCT-3′, and rat KLC-2 5′-TCTGGTGATCCAGTATGCT-3′. The target sequences of CRMP-2 and control Scramble have been described previously (41).

Hippocampal neurons from E18 rat embryos were prepared and transfected before plating, as described previously (23). In some experiments, the cotransfection of siRNA and plasmid was carried out using a calcium phosphate method before plating.

Immunofluorescence analysis. Hippocampal neurons were fixed with 3.7% formaldehyde in phosphate-buffered saline (PBS) for 10 min and treated with PBS that contained 0.05% Triton X-100 for 10 min on ice. After being washed with PBS three times, neurons were then incubated with each indicated antibody overnight at 4°C. After being washed, the samples were incubated with the appropriate Cy5-, Cy3-, or Cy2-conjugated secondary antibody. Neurons were observed using a confocal laser microscopy system (LSM 510; Carl Zeiss) built around an Axiovert 100 M system (Carl Zeiss). The delocalizations of CRMP-2, Sra-1, and WAVE1 mean more than 70% decrement of fluorescence intensity of anti-Sra-1 and WAVE1 antibodies compared to the average of those in control GST-expressing cells.

RESULTS

Interaction of CRMP-2 and Sra-1. *unc-33* encodes the *Caenorhabditis elegans* homologue of CRMPs. *unc-33* mutants show neuronal outgrowth and guidance defects in hermaphrodite-specific, sensory, and motor neurons (10, 13, 21, 34, 37). We have recently identified one of the mutation sites of *unc-33* (*e204*) which leads to defects in axon outgrowth in *C. elegans* (54a). *unc-33* (*e204*) contains the missense mutation which substitutes Asn at 389 for Asp. Asp389 in *C. elegans* corresponds to Asp71 in humans and is widely conserved in other species (Fig. 1a). Consistent with our study of *C. elegans*, we found that the expression of CRMP-2 D71N, which is the substitution of Asn at position 71 for Asp in human CRMP-2, caused the inhibition of axon outgrowth and formation in rat hippocampal neurons as will hereafter be described in detail (see Fig. 4 and 5). To elucidate the mechanism of defects in axon formation in mammalian cells, we searched for the CRMP-2-interacting proteins that this mutation affects in the binding to CRMP-2. Affinity column chromatography was performed by using CRMP-2 wild-type (WT)–and D71N–gluta-

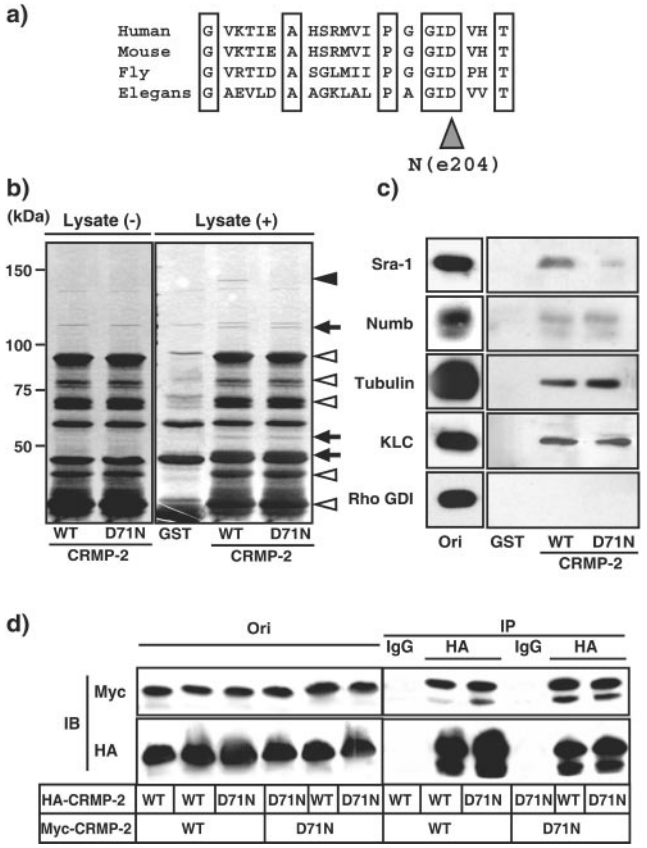

FIG. 1. Interaction of CRMP-2 D71N and CRMP-2-interacting proteins. (a) Alignments of CRMP-2 in various species. *unc-33* (e204) is one of the mutation sites of *unc-33* in *C. elegans*. (b) CRMP-2 D71N affinity chromatography. Porcine brain extract was loaded onto the column on which GST, CRMP-2 WT, or D71N-GST was immobilized. After being washed, the bound proteins were eluted by the addition of glutathione. The closed arrowhead indicates p140. The open arrowheads indicate CRMP-2–GST itself or a degradation product of CRMP-2–GST. Arrows indicate unidentified CRMP-2-interacting proteins. (c) Immunoblot analysis of known CRMP-2-interacting proteins. The elution fraction in panel b was immunoblotted with anti-Sra-1, anti-Numb, antitubulin, anti-KLC, and anti-Rho GDI antibodies. Aliquots of original samples (2% Ori) and eluates (25%) were subjected to SDS-PAGE. (d) Interaction between CRMP-2 WT and D71N. The indicated CRMP-2 plasmids were transfected into HEK293 cells. The extract of HEK293 cells in lysis buffer was incubated with anti-HA monoclonal antibody. The immunoprecipitates were analyzed by immunoblotting with anti-myc and HA monoclonal antibodies. Aliquots of original samples (1% Ori) and eluates (10%) were subjected to SDS-PAGE. IP, immunoprecipitation; IB, immunoblot.

thione *S*-transferase (GST). A 140-kDa protein (p140) specifically interacted with CRMP-2 WT, whereas this binding was decreased by the substitution of Asn at 71 for Asp in CRMP-2 (Fig. 1b, indicated by a closed arrowhead). Other CRMP-2-interacting proteins appear to bind to CRMP-2 D71N as well as CRMP-2 WT (Fig. 1b, indicated by an arrow). We identified p140 as an Sra-1 by mass spectrometry and immunoblot analysis (Fig. 1c) (14, 31). We have previously identified tubulin heterodimer, Numb, and KLC as CRMP-2-interacting molecules (16, 30, 41). We next examined the interaction between CRMP-2 D71N and these CRMP-2-interacting molecules. The binding of CRMP-2 D71N with tubulin, Numb, and KLC was comparable to that of CRMP-2 WT (Fig. 1c). In this condition, the binding of CRMP-2 D71N to Sra-1 specifically decreased compared to that of CRMP-2 WT. The immunoreactive band of Rho GDI (negative control), which is a regulator of small GTPase Rho and an abundant soluble protein, was not observed in elution fractions. It has been reported that CRMPs can form an oligomer in vitro (58). To examine whether CRMP-2 D71N forms an oligomer, a coimmunoprecipitation assay was performed by use of Myc- and hemagglutinin (HA)–CRMP-2s. When HA–CRMP-2 WT was immunoprecipitated with anti-HA antibody, Myc–CRMP-2 WT was coimmunoprecipitated with HA–CRMP-2 WT (Fig. 1d), indicating that Myc–CRMP-2 WT forms a complex with HA–CRMP-2 WT. The apparent effect of the substitution of Asn at 71 for Asp in Myc–CRMP-2 on its binding to HA–CRMP-2 WT and D71N was not observed. Taken together, these results suggest that the substitution of Asn at 71 for Asp in CRMP-2 reduces the binding only to Sra-1 under our conditions.

To examine whether CRMP-2 forms the complex with Sra-1 in vivo, a coimmunoprecipitation assay was performed. Sra-1 was reciprocally coimmunoprecipitated with CRMP-2 but not with Rho GDI (negative control) (Fig. 2a). When CRMP-2 was immunoprecipitated with the anti-CRMP-2 antibody, the amount of Sra-1 coimmunoprecipitated with CRMP-2 was small. This might be explained by the fact that the amount of Sra-1 expressed in hippocampal neurons is about 30 times smaller than that of CRMP-2. To confirm the direct interaction between CRMP-2 and Sra-1, an in vitro binding assay was performed. Purified Sra-1 directly interacted with CRMP-2 WT-GST but not with control GST (Fig. 2b). Consistent with the result of affinity column chromatography, this binding was decreased by the substitution at position 71 in CRMP-2. Taken together, these results indicate that CRMP-2 physiologically and directly interacts with Sra-1. We performed an in vitro binding assay to narrow down the binding region of Sra-1 on CRMP-2 (Fig. 2c). Sra-1 was observed in the elution fraction from CRMP-2 ΔN348 and ΔN440, indicating that the C-terminal region of CRMP-2 interacts with Sra-1. We narrowed down the binding region of CRMP-2 on Sra-1 (Fig. 2d). CRMP-2 was observed in the elution fraction from Sra-1 801-1253, indicating that the C-terminal region of Sra-1 interacts with CRMP-2.

Localization of Sra-1 and WAVE1 in hippocampal neurons. We and others have previously reported that Sra-1/CYFIP1 is a specific effector for small GTPase Rac1 and directly interacts with filamentous actin (31, 46). Sra-2/PIR121/CYFIP2 is an isoform of Sra-1 (14, 46). Increasing evidence has shown that Sra-1 or Sra-2 forms a tight complex with WAVE1, Nap-1, Abi-2, and HSPC300 and is essential for the reorganization of actin cytoskeleton downstream of Rac (14, 25, 49). We examined the localization of Sra-1 and WAVE1 in rat cultured hippocampal neurons. The hippocampal neuron extends several minor processes during the first 12 to 24 h after plating (stages 1 and 2) (11). One of the processes then begins to extend rapidly to form an axon (stage 3). The remaining processes acquire the morphological features of dendrites thereafter (stage 4). The results of immunocytochemical analysis showed that Sra-1 and WAVE1 were localized in the growth cones of minor processes at stage 2 neurons (Fig. 3a). The

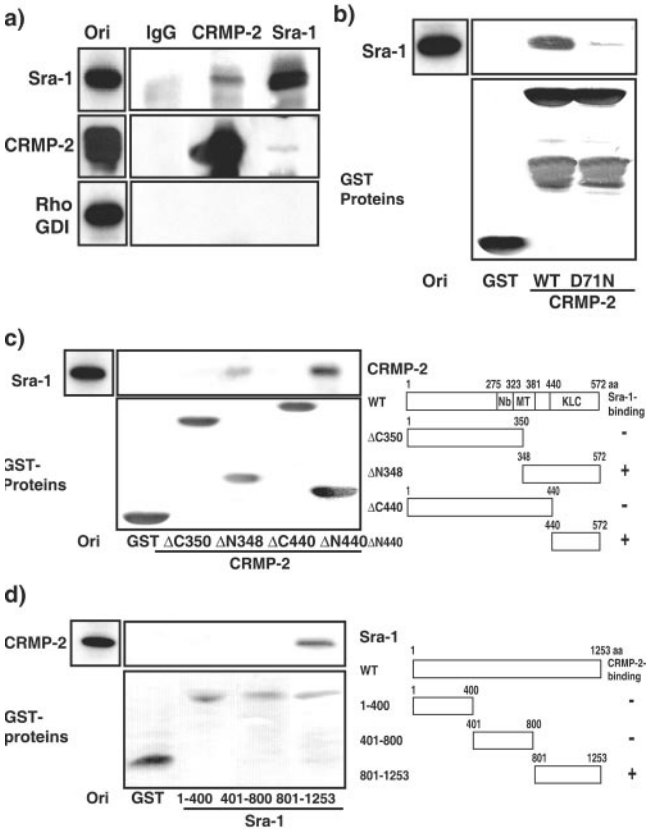

FIG. 2. Interaction of CRMP-2 D71N and Sra-1. (a) Coimmunoprecipitation of CRMP-2 with Sra-1. The porcine brain extract in lysis buffer was incubated with anti–CRMP-2 polyclonal or anti-Sra-1 antibody. The immunoprecipitates were analyzed by immunoblotting with anti-Sra-1, anti-CRMP-2 monoclonal, and anti-Rho GDI antibodies. Aliquots of original samples (2% Ori) and eluates (25%) were subjected to SDS-PAGE. (b) Direct interaction of CRMP-2 WT or D71N with Sra-1. GST and CRMP-2 WT or D71N-GST immobilized beads were incubated with purified Myc–Sra-1. After being washed, the bound proteins were eluted by the addition of glutathione and analyzed by silver staining. Aliquots of original samples (1% Ori) and eluates (25%) were subjected to SDS-PAGE. (c) The Sra-1-binding region on CRMP-2. GST protein immobilized beads were incubated with porcine brain extract. After being washed, the bound proteins were eluted by the addition of glutathione and immunoblotted with anti-Sra-1 antibody (upper panel). Aliquots of original samples (2% Ori) and eluates (10%) were subjected to SDS-PAGE. The domain structure of various CRMP-2 fragments is represented. Nb, Numb-binding region (aa 275 to 323); MT, microtubule assembly region (aa 323 to 381); KLC, KLC-binding region (aa 440 to 572). (d) The CRMP-2-binding region on Sra-1. GST protein immobilized beads were incubated with His-CRMP-2. After being washed, the bound proteins were eluted by the addition of glutathione and immunoblotted with anti-CRMP-2 monoclonal antibody (upper panel). The domain structure of various Sra-1 fragments is represented. Aliquots of original samples (2% Ori) and eluates (10%) were subjected to SDS-PAGE.

immunoreactivity of Sra-1 was high in the cell body and the growth cone of developing axon but low in the shaft of the axon and in minor processes in stage 3 neurons. This localization was similar to the localization of WAVE1. We have previously found that CRMP-2 accumulates in the growth cones and distal parts of growing axons during stage 3 (23). Double immunostaining of Sra-1 and CRMP-2 showed that CRMP-2 and Sra-1 were strongly colocalized only in the growth cone of axon (Fig. 3b, images 1) but not in the growth cones of minor processes (Fig. 3b, images 2 and 3). The high-magnification view in the growth cone of the axon revealed that Sra-1 and WAVE1 were localized in both the central and peripheral regions of the growth cone (Fig. 3c). CRMP-2 was relatively concentrated in the central region of the growth cone and was colocalized strongly with Sra-1 or WAVE1 in the central region and slightly with Sra-1 or WAVE1 in the peripheral region, where filamentous actin accumulated (Fig. 3c, arrowheads). Interestingly, Sra-1 and WAVE1 were observed in the tip of filopodia, but CRMP-2 was not.

CRMP-2-induced axon outgrowth requires Sra-1 and WAVE1. To evaluate the physiological meaning of the interaction between CRMP-2 and Sra-1 in axon outgrowth, neurons were transfected with CRMP-2 D71N and Sra-1 and the neurons were fixed at DIV3, when one of the minor processes acquires axonal character and elongates rapidly. The length of the primary axon of the cells expressing CRMP-2 WT was significantly longer than that of the cells expressing GST, as reported previously (Fig. 4a and b) (16). CRMP-2 D71N and ΔN440, which contains the KLC- and Sra-1-binding regions, suppressed axon outgrowth, which suggests that CRMP-2 D71N and ΔN440 serve as dominant-negative forms. The apparent effect of the expression of Sra-1 on axon outgrowth was not observed, whereas Sra-1 801-1253, which contains the CRMP-2-binding region, inhibited it. WAVE1 WT and the dominant-negative form of WAVE1 (WAVE1 DN) inhibited axon outgrowth. WAVE1 DN lacking the V domain cannot bind to actin. To examine whether CRMP-2 promotes axon outgrowth via the Sra-1/WAVE1 complex, the cotransfection with CRMP-2 and Sra-1 801-1253 or WAVE1 DN was performed. CRMP-2-induced axon outgrowth was inhibited by the coexpression of Sra-1 801-1253 or WAVE1 DN (Fig. 4c).

We used RNAi to examine the functions of endogenous Sra-1, WAVE1, and KLC. The results of immunoblot analysis revealed that Sra-1-, WAVE1-, and KLC 1 and 2 (KLCs)-specific small interfering RNAs (siRNAs) efficiently knocked down their expression in rat embryonic fibroblast 3Y1 cells (see Fig. S1a in the supplemental material), whereas the expression levels of actin as a control protein did not change among them. The knockdown of Sra-1 and WAVE1 inhibited insulin-induced membrane ruffling at the cell periphery (Fig. S1b and S1c). These results indicate that these siRNAs are useful for investigating the function of endogenous Sra-1, WAVE1, and KLCs in rat cells. We used RNAi to test whether endogenous Sra-1 and WAVE1 are required for axon outgrowth (Fig. 4d). We have previously found that the knockdown of CRMP-2 causes the inhibition of axon outgrowth (41, 60). The knockdown of Sra-1 and WAVE1 also inhibited axon outgrowth compared to Scramble, which is an siRNA that presents no homology with any human, mouse, and rat mRNAs. These effects were rescued by the expression of RNAi-resistant CRMP-2 and Sra-1 (RrCRMP-2 and RrSra-1) (Fig. 4d), indicating that the knockdown effects are specific for CRMP-2 and Sra-1. We could not rescue the inhibitory effects of WAVE1 siRNA by the expression of RrWAVE1 (data not shown). The failure of rescue of WAVE1 experiments might be due to its ability to induce the formation of abnormal actin

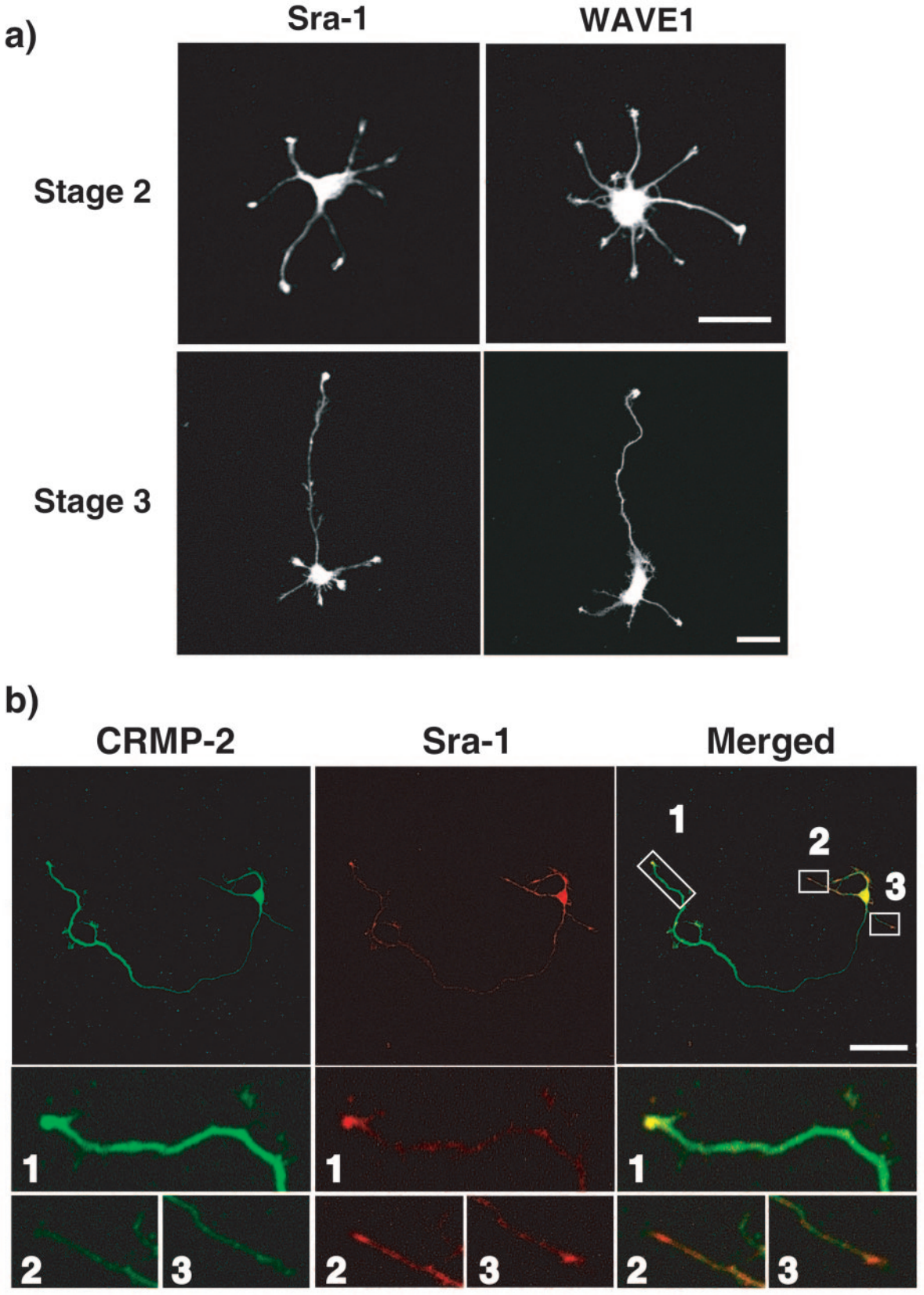

FIG. 3. Localization of Sra-1 and WAVE1 in hippocampal neurons. (a) Localization of Sra-1 and WAVE1. Neurons were stained with anti-Sra-1 or anti-WAVE1 polyclonal antibody at stage 2 (DIV1) and stage 3 (DIV3). (b) Colocalization of Sra-1 and CRMP-2 at the growth cone of the axon in DIV3 neurons. Neurons were double stained with anti-CRMP-2 (green) monoclonal and anti-Sra-1 (red) antibodies. The enlarged images of the growth cone of the axon (1) and remaining minor processes (2 and 3) are shown. Bar, 20 μm. (c) Localization of Sra-1 and WAVE1 in the growth cone of the axon. Neurons were stained with anti-CRMP-2 (green) monoclonal, anti-Sra-1, or anti-WAVE1 (red) antibody as well as Cy5-phalloidin (Blue). The enlarged images of the framed rectangles are shown at the right side.

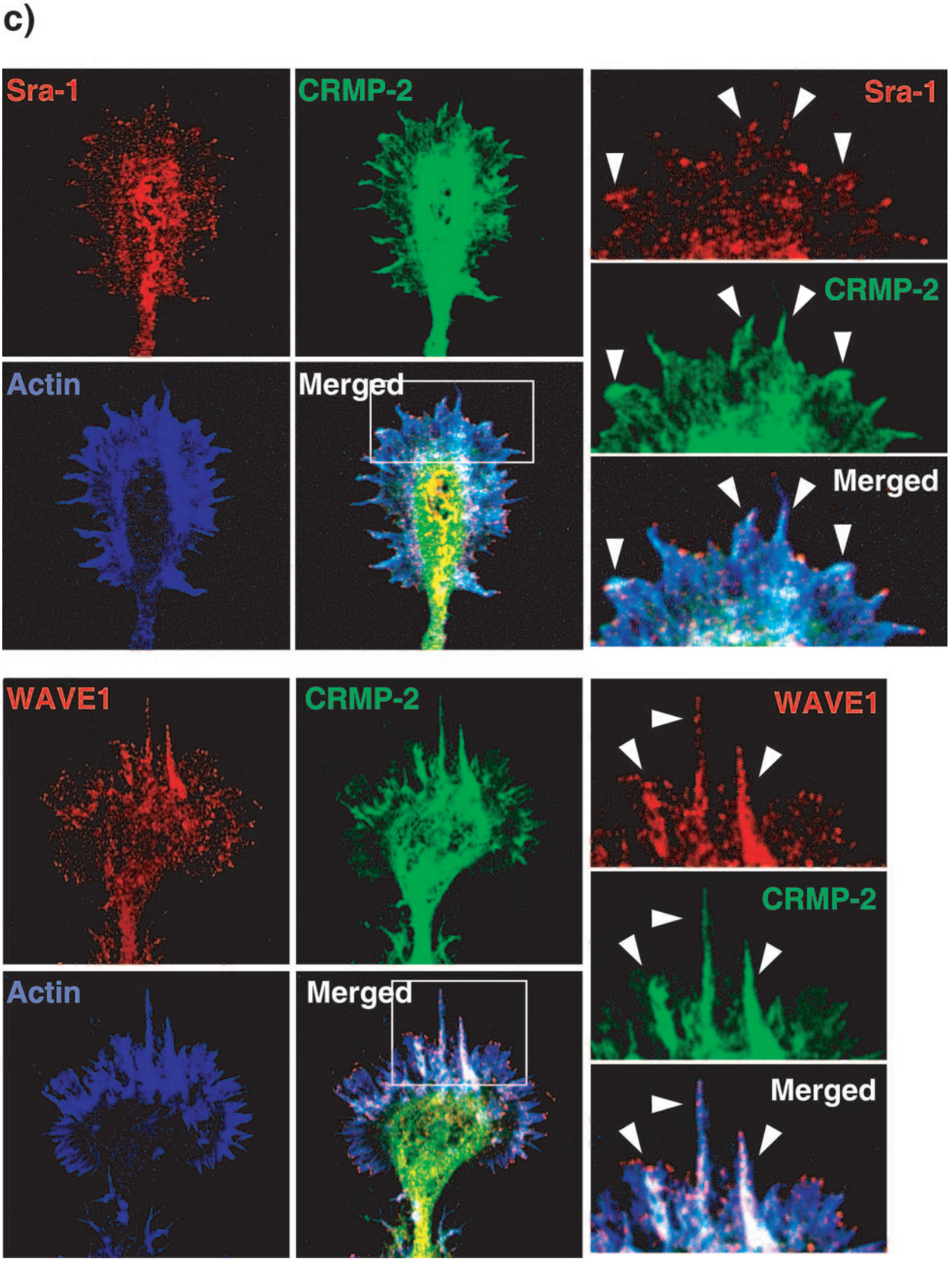

FIG. 3—*Continued.*

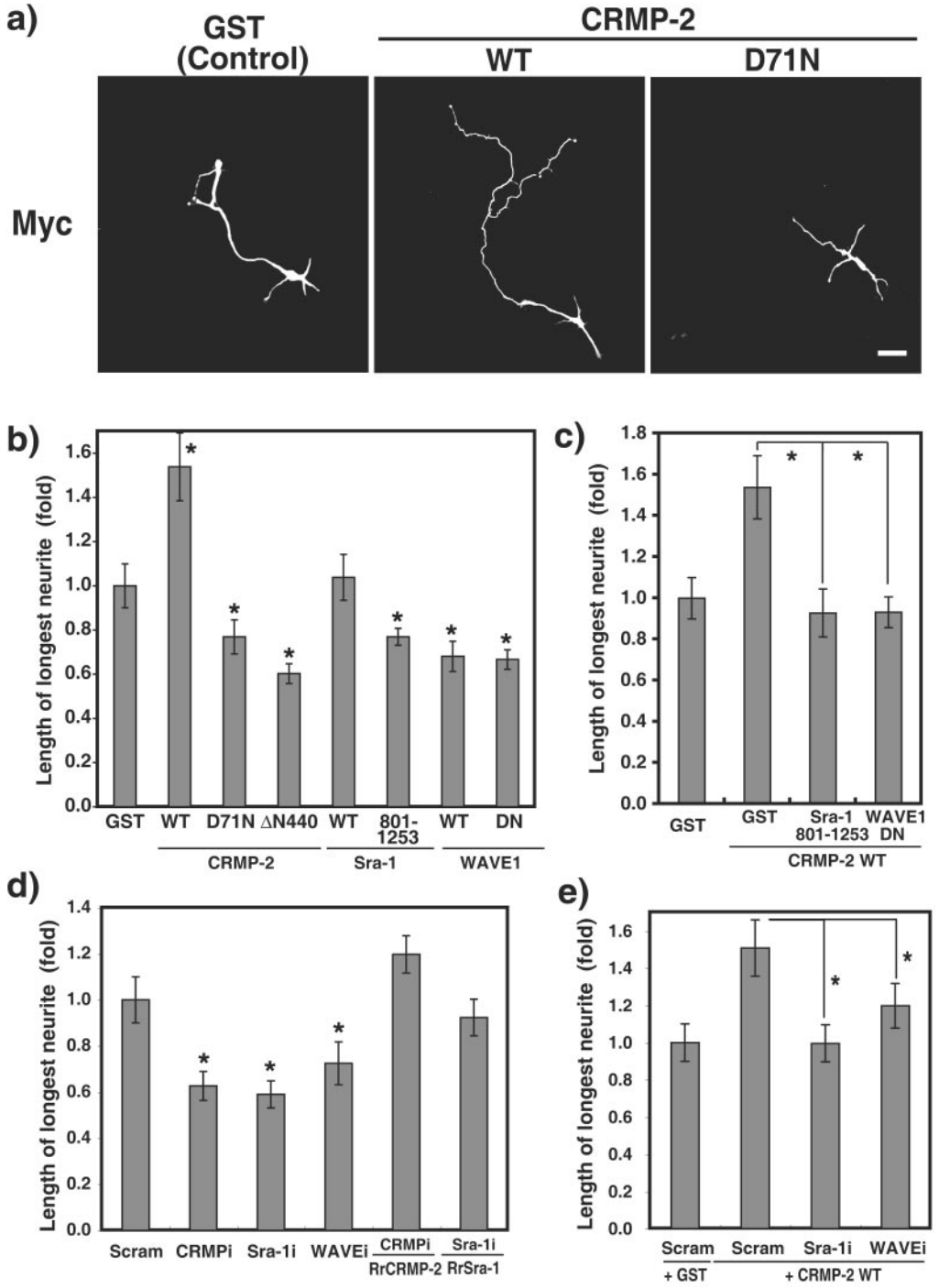

FIG. 4. CRMP-2-induced axon outgrowth requires Sra-1 and WAVE1. (a) Effect of CRMP-2 D71N on axon outgrowth. pCAGGS-myc-GST, CRMP-2 WT, or CRMP-2 D71N was transfected into hippocampal neurons. Transfected cells were stained with anti-myc antibody at DIV3. (b and c) Effect of CRMP-2, Sra-1, and WAVE1 on axon outgrowth. The longest neurite was considered an axon. Axon length was measured on DIV3 neurons transfected with the indicated plasmid. WAVE1 DN lacks the V domain and serves as a dominant-negative form. (d and e) Effect of knockdown of Sra-1 and WAVE1 on the CRMP-2-induced axon outgrowth. The indicated Cy3-labeled siRNA and pCAGGS-myc-GST, CRMP-2 WT, RNAi-resistant CRMP-2 WT (RrCRMP-2), or RrSra-1 WT were cotransfected into hippocampal neurons. More than 80% of the cells transfected with Myc-GST or CRMP-2 were Cy3 siRNA positive. Axon length was measured by anti-myc antibody staining on DIV3 neurons. The data are means ± standard deviations of at least three independent experiments. Asterisks indicate the difference from the value of GST at $P < 0.05$ (Student's t test). $n > 150$. Bar, 20 μm. Scram, Scramble. CRMPi, Sra-1i, and WAVEi, interference of CRMP, Sra-1, and WAVE, respectively, by siRNA.

filament clusters. Taken together, these results indicate that CRMP-2, Sra-1, and WAVE1 are required for axon outgrowth. It seems that the effect of knockdown of WAVE1 was weaker than that of expression of WAVE1 DN (Fig. 4). These results might be due to the redundant expression of WAVE isoforms in brain (52). The cotransfection of CRMP-2 WT and siRNA of Sra-1 or WAVE1 was performed next (Fig. 4e). The CRMP-2-induced axon outgrowth was suppressed by the knockdown of Sra-1 or WAVE1, suggesting that CRMP-2-induced axon outgrowth requires Sra-1 and WAVE1.

CRMP-2-induced axon formation requires Sra-1 and WAVE1. We have previously shown that the overexpression of CRMP-2 induces the formation of multiple axons (23). We compared the effect of CRMP-2 WT and D71N on axon formation at DIV6. To visualize secondary axons, neurons at DIV6 are better than those at DIV3, because the secondary axons appear later (60). Some CRMP-2 WT-expressing neurons bore multiple axons (Fig. 5a). The processes exhibited the typical characteristic morphology of axons. They were long and thin and were branched at right angles. Furthermore, the processes were immunostained by the axonal markers Tau-1 and anti-synapsin 1 antibodies (Fig. 5a; see Fig. S2 in the supplemental material) but were immunonegative for the somatodendritic marker protein MAP-2 (data not shown). On the other hand, the neurons expressing CRMP-2 D71N had a short single axon. In addition, it should be noted that some of the neurons transfected with CRMP-2 D71N bore no axon (Fig. 5a). The processes were immunonegative for Tau-1 but were immunostained by anti-MAP2 antibody (see Fig. S2 in the supplemental material). Statistical analysis revealed that the expression of CRMP-2 WT increased the percentage of neurons bearing multiple axons and decreased that of neurons bearing single and no axon (Fig. 5b). On the other hand, the expression of CRMP-2 D71N and ΔN440 increased the percentage of neurons bearing no axon and decreased that of neurons bearing single and multiple axons. The apparent effect of the expression of Sra-1 on axon formation was not observed, whereas the expression of Sra-1 801-1253 increased the percentage of neurons bearing no axon. These results suggest that the interaction between CRMP-2 and Sra-1 is important for axon formation. The expression of WAVE1 WT and WAVE1 DN increased the percentage of neurons bearing no axon. We used RNAi to examine the effect of endogenous CRMP-2, Sra-1, and WAVE1 on axon formation (Fig. 5b). The knockdown of CRMP-2, Sra-1, and WAVE1 increased the percentage of neurons without axons and decreased that of neurons bearing single axons and multiple axons compared to levels for control Scramble. This result indicates that CRMP-2, Sra-1, and WAVE1 are required for axon formation. We also examined whether the knockdown of Sra-1 or WAVE1 affected the number or length of minor processes and dendrite formation (see Fig. S3 in the supplemental material). We found that the knockdown of Sra-1 or WAVE1 slightly decreased the number or length of minor processes, but the statistical differences were not observed at DIV3. The knockdown of Sra-1 or WAVE1 inhibited dendrite formation at DIV6. Sra-1 and WAVE1 seem to be required for dendrite formation. To examine whether CRMP-2 induces supernumerary axon formation via Sra-1 and WAVE1, the cotransfection of CRMP-2 WT and Sra-1 801-1253 or WAVE1 DN was performed (Fig. 5c). The CRMP-2-induced multiple-axon formation was suppressed by the expression of Sra-1 801-1253 or WAVE1 DN. The consistent result was obtained in the knockdown of Sra-1 and WAVE1. Taken together, these results suggest that CRMP-2-induced axon formation requires Sra-1 and WAVE1.

CRMP-2 links kinesin-1 to Sra-1 and WAVE1. In the present study, we found that the interaction of CRMP-2 with Sra-1 is important for axon formation. How does CRMP-2 regulate axon formation via the Sra-1/WAVE1 complex? We have recently found that CRMP-2 directly interacts with KLC (30). CRMP-2 is transported by kinesin-1 and accumulates at the distal part of axons. These findings raise the possibility that CRMP-2 links kinesin-1 to the Sra-1/WAVE1 complex and transports the Sra-1/WAVE1 complex to the tip of axons. To address this possibility, the complex formation of kinesin-1/CRMP-2/Sra-1/WAVE1 was examined. When CRMP-2 was immunoprecipitated with anti-CRMP-2 antibody, the immunoreactive bands of Sra-1, WAVE1, and KLC were detected in the immunoprecipitate (Fig. 6a). The immunoreactive band of Rho GDI (negative control) was not detected. The stoichiometry of CRMP-2 to KLC, Sra-1, or WAVE1 was about 0.2, 0.1, or 0.1, respectively. To examine whether kinesin-1 interacts with the Sra-1/WAVE1 complex via CRMP-2, we performed a GST-KLC pull-down assay by using HEK293 lysates (Fig. 6b). We found that Sra-1 formed a complex with WAVE1 in HEK293 cells (see Fig. S4 in the supplemental material) and that the expression of endogenous CRMP-2 was hardly detected (Fig. 6b). In the absence of CRMP-2, the interaction of GST-KLC with Sra-1 and WAVE1 was not observed. When HA-CRMP-2 was expressed in HEK293 cells, the interaction of GST-KLC with Sra-1 and WAVE1 was observed. Taken together, these results suggest that CRMP-2 links kinesin-1 to Sra-1 and WAVE1.

CRMP-2-dependent localization of Sra-1 and WAVE1 at the growth cones of axons. We found that CRMP-2 D71N lowers its activity to interact with Sra-1 but not with KLC (Fig. 1). Thus, it is possible that the expression of CRMP-2 D71N perturbs the interaction between endogenous CRMP-2 and kinesin-1, thereby resulting in the delocalization of the Sra-1/WAVE1 complex from the growth cones of axons. We examined the effect of the expression of CRMP-2 D71N on the localization of Sra-1 and WAVE1 at the tip of growing axons at DIV3. The accumulation of Sra-1 in the growth cones of axons was observed in the neurons transfected with control GST and CRMP-2 WT, whereas the ectopic expression of CRMP-2 D71N and ΔN440 inhibited axon outgrowth and caused the delocalization of Sra-1 from the tip of axons (Fig. 7a and b). The effect of CRMP-2 D71N on minor processes appears to be less than that on axons. Similar results were obtained with WAVE1 (Fig. 7b). The delocalization of Sra-1 by CRMP-2 D71N is not dependent on the reduction of the size of the growth cones. We quantitatively examined the delocalization of Sra-1 by staining between anti-Sra-1 antibody and BODIPY630, a cytosol marker (see Fig. S5 in the supplemental material). The expression of CRMP-2 D71N reduced the fluorescence ratio of Sra-1/BODIPY630, indicating that the expression of CRMP-2 D71N delocalizes Sra-1 from the growth cones of axons. We examined these results by using RNAi to test whether endogenous CRMP-2 is required for the accumulation of Sra-1 at the tip of growing axons. Consistent

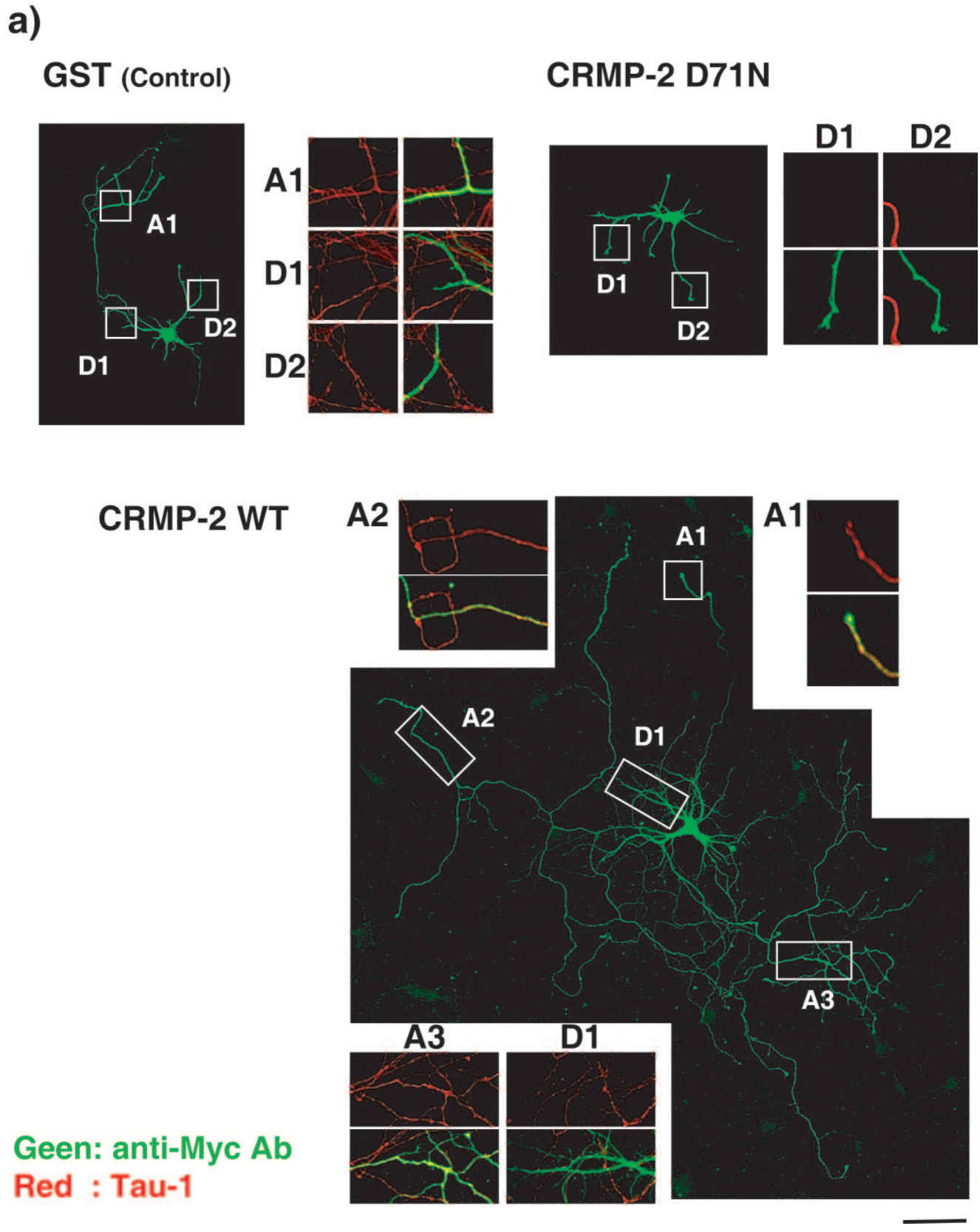
a)
GST (Control)
A1
D2
D1
A1
D1
D2
CRMP-2 D71N
D1
D2
D1
D2
CRMP-2 WT
A2
A1
A1
A2
D1
A3
A3
D1
Geen: anti-Myc Ab
Red : Tau-1

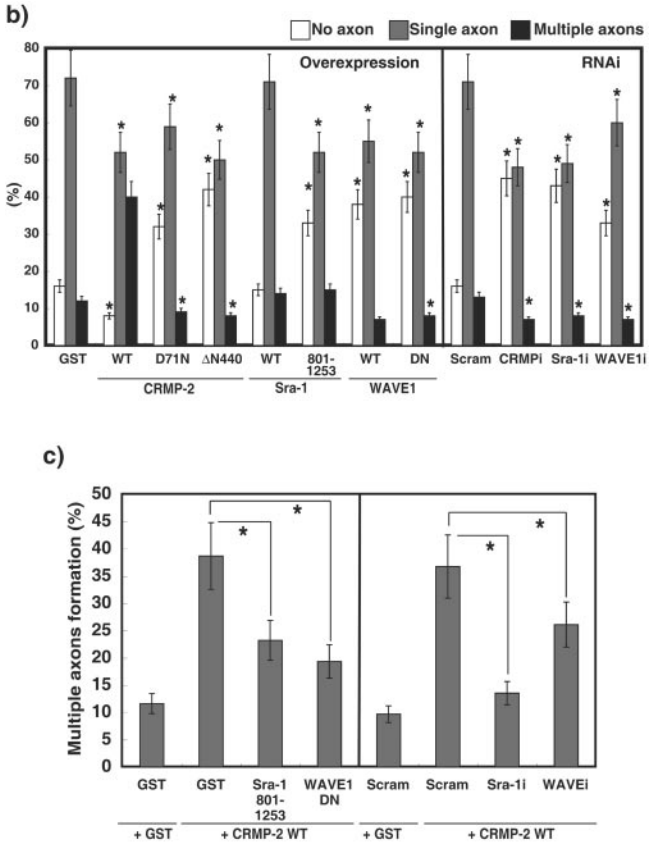

FIG. 5. CRMP-2-induced axon formation requires Sra-1 and WAVE1. (a) Effect of CRMP-2 D71N on axon formation. The indicated plasmid was transfected into hippocampal neurons. Neurons were double stained with anti-myc (green) monoclonal and anti-Tau-1 (red) antibodies at DIV6. The morphology of neurons was visualized by anti-myc antibody staining (green). The enlarged images of double staining with anti-myc (green) and anti-Tau-1 (red) antibodies in axons (A1 to A3) and dendrites (D1 and D2) are shown. These figures show the representative cells expressing GST with a single axon, CRMP-2 WT with multiple axons, and CRMP-2 D71N without axons. (b) Effect of Sra-1 and WAVE1 on axon formation. The indicated plasmid (overexpression) or Cy3-labeled siRNA and pCAGGS-myc-GST (RNAi) were transfected into hippocampal neurons. More than 80% of the cells transfected with Myc-GST were Cy3-siRNA positive. Neurons were double-stained with anti-myc monoclonal and anti-Tau-1 antibodies at DIV6. The percentages of no axon, single axon, and multiple axons were estimated. The morphology of neurons was traced by anti-myc antibody staining. Axons were determined by Tau-1 staining (axon marker) and its morphology (11). (c) Effect of knockdown of Sra-1 and WAVE1 on CRMP-2-induced multiple axon formation. The indicated Cy3-labeled siRNA and pCAGGS-myc-GST or CRMP-2 WT were cotransfected into hippocampal neurons. More than 80% of the cells transfected with Myc-GST or Myc–CRMP-2 were Cy3-siRNA positive. Neurons were double stained with anti-myc monoclonal and anti-Tau-1 antibodies at DIV6. The percentages of no axon, single axon, and multiple axons were estimated. The morphology of neurons was traced by anti-myc antibody staining. Axons were determined by Tau-1 staining (axon marker) and its morphology (11). The data are means ± standard deviations of at least three independent experiments. Asterisks indicate the difference from the value of GST or Scramble at $P < 0.05$ (Student's t test). $n > 150$. Bar, 100 μm. Ab, antibody.

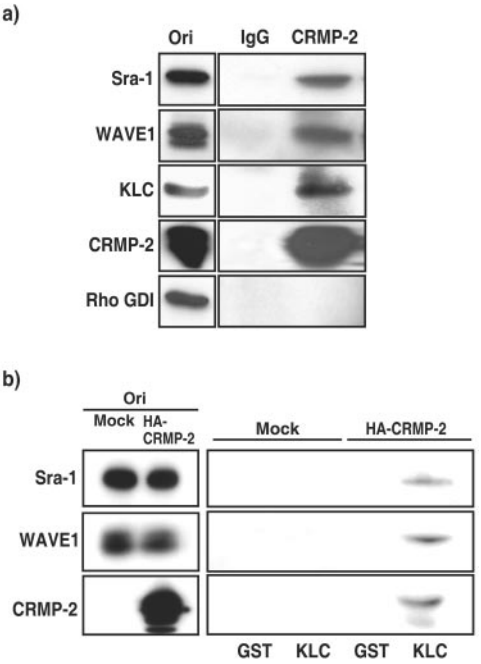

FIG. 6. CRMP-2 links kinesin-1 to Sra-1 and WAVE1. (a) Coimmunoprecipitation of CRMP-2 with KLC, Sra-1, and WAVE1. The porcine brain extract was incubated with anti-CRMP-2 polyclonal antibody. The immunoprecipitates were analyzed by immunoblotting with anti-Sra-1, anti-WAVE1 monoclonal, anti-KLC, and anti-Rho GDI antibodies. Aliquots of original samples (2% Ori) and eluates (25%) were subjected to SDS-PAGE. (b) Pull-down assay of KLC. HEK293 lysates with or without transfection with pCAGGS-HA-CRMP-2 WT were loaded onto the beads on which GST or GST-KLC TPR was immobilized. After being washed, the bound proteins were eluted by addition of glutathione. The elution fractions were immunoblotted with anti-Sra-1 polyclonal, anti-WAVE1 monoclonal, and anti-HA monoclonal antibodies. Aliquots of original samples (2% Ori) and eluates (10%) were subjected to SDS-PAGE.

with the data on the expression of CRMP-2 D71N and ΔN440, the knockdown of CRMP-2 evoked the delocalization of Sra-1 and WAVE1 from the tip of axons (Fig. 7c). These results suggest that CRMP-2 is important for the accumulation of Sra-1 and WAVE1 in the growth cones of axons.

Kinesin-1-dependent localization of CRMP-2, Sra-1, and WAVE1 at the growth cones of axons. We examined by using RNAi whether endogenous kinesin-1 is required for the accumulation of Sra-1 and WAVE1 at the tip of growing axons. The knockdown of KLC 1 and 2 (KLCs) suppressed axon outgrowth (see Fig. S6 in the supplemental material) and perturbed the accumulation of CRMP-2 at the distal part and the growth cones of axons at DIV3 (Fig. 8a and b). In this condition, the delocalization of Sra-1 and WAVE1 from the tip of axons was also observed. Kinesin-1 is composed of KIF5 (or KHC) and KLC. We further tested the fragments of KIF5A headless (HL), which lacks its motor domain and serves as a dominant-negative form of kinesin-1 (7, 44). The expression of KIF5A HL suppressed axon outgrowth (Fig. S6) and perturbed the accumulation of CRMP-2, Sra-1, and WAVE1 at the distal part and the growth cones of axons (Fig. 8c). Taken together, these findings suggest that kinesin-1 is important for the accu-

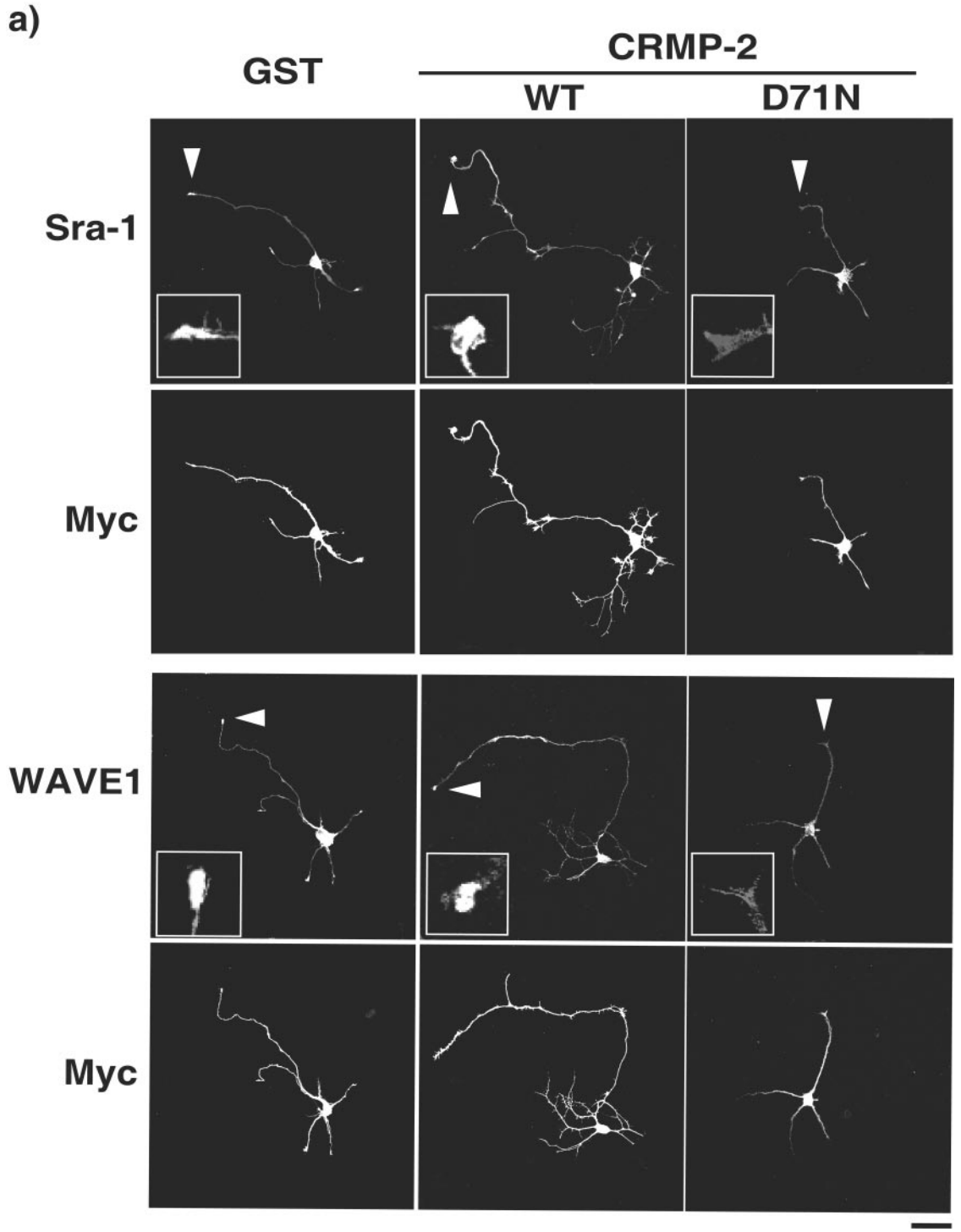

FIG. 7. CRMP-2-dependent localization of Sra-1 and WAVE1 at the growth cones of axons. (a and b) Effect of expression of CRMP-2 D71N on the localization of Sra-1 and WAVE1 at the growth cones of axons. pCAGGS-myc-GST, CRMP-2 WT, CRMP-2 D71N, or CRMP-2 ΔN440 was transfected into hippocampal neurons. Transfected cells were stained with anti-myc monoclonal and anti-Sra-1 or anti-WAVE1 polyclonal antibodies. The percentage of accumulation of Sra-1 and WAVE1 at the growth cones of axons was estimated. (c) Effect of the knockdown of CRMP-2 on the localization of Sra-1 and WAVE1 at the growth cones of axons. The indicated Cy3-labeled siRNA and pCAGGS-myc-GST were cotransfected into hippocampal neurons. More than 80% of the cells transfected with Myc-GST were Cy3-siRNA positive. Transfected cells were stained with anti-myc monoclonal and anti-Sra-1 or anti-WAVE1 polyclonal antibody at DIV3. The accumulation of Sra-1 and WAVE1 at the growth cones of axons was estimated. The data are means ± standard deviations of at least three independent experiments. Asterisks indicate the difference from the value of GST at $P < 0.05$ (Student's t test). $n > 150$. Bar, 20 μm.

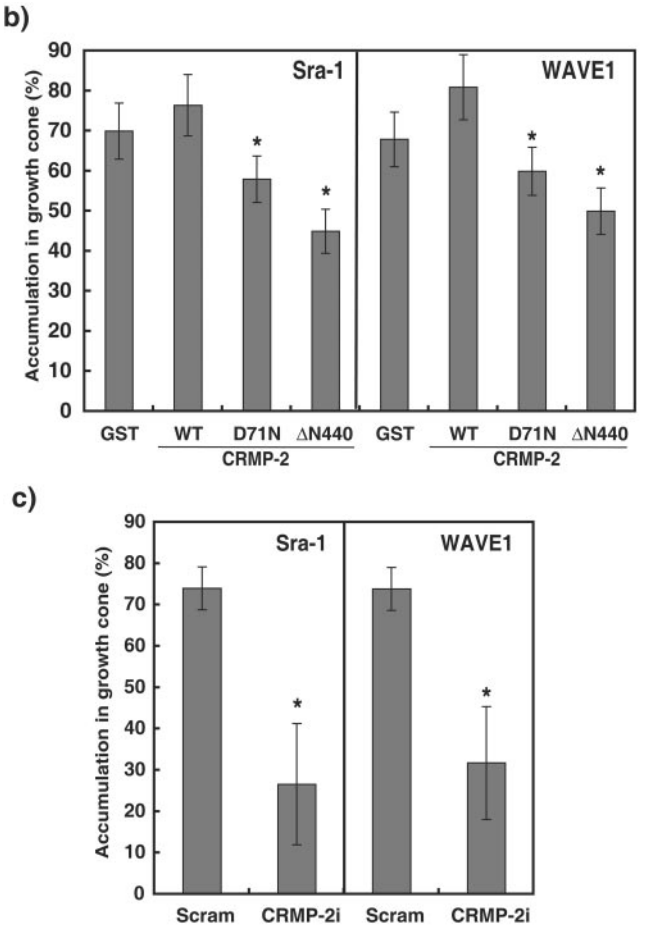

FIG. 7—*Continued.*

mulation of CRMP-2, Sra-1, and WAVE1 in growth cones of axons.

DISCUSSION

Interaction of CRMP-2 with Sra-1. In the present study, we found that CRMP-2 directly and physiologically interacted with Sra-1 (Fig. 2). We have previously reported that aa 275 to 323 and 440 to 572 of CRMP-2 interact with Numb and KLC, respectively, and that aa 323 to 381 of CRMP-2 enhances microtubules assembly (16, 30, 41) (Fig. 2c). We also found that the C-terminal region of Sra-1 directly interacted with the C-terminal region of CRMP-2, which overlaps with the KLC-binding region (Fig. 2; see Fig. S7 in the supplemental material) (30). We constructed additional deletion fragments, but we could not distinguish between the Sra-1- and KLC-binding regions within the C-terminal region of CRMP-2 (data not shown). It is, however, worth noting that KLC did not compete with the binding of Sra-1 to CRMP-2 in vitro (data not shown). Thus, CRMP-2 can link KLC to Sra-1 (Fig. 6b). The substitution of Asn at position 71 for Asp in CRMP-2 reduced the binding to Sra-1 but not to other CRMP-2-interacting molecules under our conditions (Fig. 1). Sra-1 appears to be associated with CRMP-2 in a manner different from other CRMP-2-interacting molecules.

How does the substitution of Asn at 71 for Asp in CRMP-2 affect its binding activity to Sra-1? Recently, a three-dimensional structure of CRMP-1, which is an isoform of CRMP-2, has been reported (12). CRMP-1 assumes a bilobed "lung-shaped" structure and constitutes the upper and lower lobes. The upper lobe is composed of the N-terminal β-sheet (aa 15 to 69) domain. The lower lobe is composed of the C-terminal α/β barrel (aa 70 to 490) domain. Unfortunately, the structure of CRMP-1 at the C-terminal region is unsolved, because the C-terminal region is proteolytically susceptible. Based on our homology modeling, Asp at 71 in CRMP-2 appears to locate in the hinge between these two domains (data not shown). Because the upper lobe interacts with the lower lobe via hydrogen bonding, it is possible that the substitution of Asn at 71 for Asp in CRMP-2 affects the topology of its C-terminal region, thereby reducing its binding activity to Sra-1. The exact difference of structure between CRMP-2 WT and D71N is unknown. Further study is necessary to elucidate the mode of action of CRMP-2 D71N.

We have recently found that glycogen synthase kinase 3β phosphorylates CRMP-2 at Thr-514 downstream of the phosphatidylinositol 3-kinase–Akt pathway, thereby regulating neuronal polarity (60). Since tubulin less efficiently interacts with phosphomimic CRMP-2 (CRMP-2 T514D), in which Thr-514 was replaced by Asp, the phosphorylation of CRMP-2 at T514 appears to lower its activity to interact with tubulin. We compared the binding activity of Sra-1 and tubulin to CRMP-2 WT and T514D and found that tubulin interacted with CRMP-2 T514D less efficiently than with CRMP-2 WT, whereas Sra-1 interacted with CRMP-2 T514D as well as CRMP-2 WT (see Fig. S8 in the supplemental material).

The role of the Sra-1/WAVE1 complex in axon formation. Sra-1 and WAVE1 were localized in the growth cone of minor processes of stage 2 neurons (Fig. 3a). We also found that Sra-1 and WAVE1 were localized in the growth cone of not only developing axons but also other minor processes of stage 3 neurons under the conditions where CRMP-2 accumulated at the growth cone in developing axons (Fig. 3b). We think that both the localization and the activation of Sra-1 and WAVE1 are important for axon formation. Sra-1 and WAVE1 are downstream effectors of Rac. It has been reported that Rac, Sra-1, and WAVE1 are involved in axon formation in *Drosophila melanogaster* (19, 45, 61). We and others have shown that the PAR complex, including PAR-3, PAR-6, and an atypical PKC (aPKC), accumulates at the growth cone of the developing axons during the transition from stage 2 to stage 3 and regulates axon specification (42, 47). We have recently found that STEF/Tiam1, a Rac-specific guanine nucleotide exchange factor (GEF), accumulates at the growth cone of the developing axon and promotes axon formation downstream of the PAR complex (43). The spatiotemporal activation of Sra-1 and WAVE1 by PAR-STEF-Rac signaling in the growth cone of one of the minor processes may partly account for axon formation.

The Sra-1/WAVE1 complex is known to play a critical role in actin polymerization and the formation of lamellipodia by relaying activation signals from Rac to the actin-nucleating complex Arp2/3 (14, 49, 50). Strasser et al. have demonstrated that the inhibition of the Arp2/3 complex by overexpression of the CA domain of N-WASP, which interacts with the Arp2/3

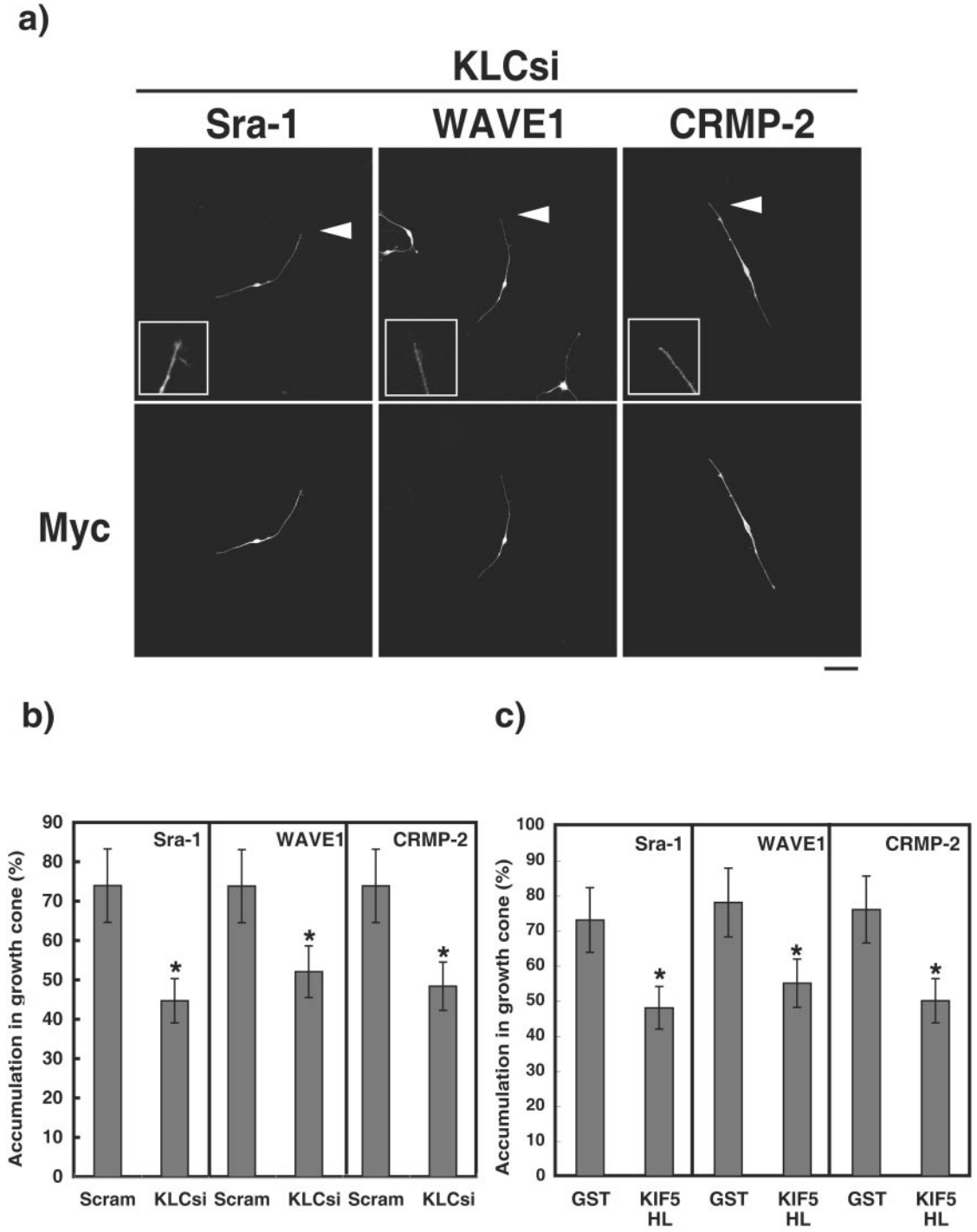

FIG. 8. Kinesin-1-dependent localization of CRMP-2 and Sra-1 and WAVE1 at the growth cones of axons. (a and b) Effect of knockdown of KLCs on the localization of Sra-1, WAVE1, and CRMP-2 at the growth cones of axons. The Cy3-labeled siRNA of Scramble or KLCs and pCAGGS-myc-GST was cotransfected into hippocampal neurons. More than 80% of the cells transfected with Myc-GST were Cy3-siRNA positive. Transfected cells were stained with anti-myc monoclonal and anti-CRMP-2, anti-Sra-1, or anti-WAVE1 polyclonal antibody. The accumulation of CRMP-2, Sra-1, and WAVE1 at the growth cones of axons was estimated at DIV3. (c) Effect of the expression of KIF5 headless (HL) on the localization of Sra-1, WAVE1, or CRMP-2 at the growth cones. pCAGGS-myc-KIF5 HL was cotransfected into hippocampal neurons. Transfected cells were stained with anti-myc and anti-CRMP-2 monoclonal, anti-Sra-1, or anti-WAVE1 polyclonal antibody at DIV3. The accumulation of CRMP-2, Sra-1, and WAVE1 at the growth cones of axons was estimated at DIV3. The data are means ± standard deviations of at least three independent experiments. Asterisks indicate the difference from the value of GST at $P < 0.05$ (Student's t test). $n > 150$. Bar, 20 μm. Scram, Scramble. KLCsi, interference of KLC1 and KLC2 (KLCs) by siRNA.

complex, enhances axon outgrowth (51). Their observations are apparently inconsistent with our findings. We used the full-length WAVE1 mutant lacking the actin-binding domain (V domain). Our mutant is expected to bind to other WAVE1 ligands such as Abl, profilin, WRP, and Abi-1, not just Arp2/3 (14, 38, 48, 59). This WAVE1 mutant could sequester multiple WAVE1 ligands, including Arp2/3. In this scenario, the overexpression of WAVE1 WT produced an effect similar to that of our WAVE1 mutant (Fig. 4 and 5). WAVE1 appears to regulate axon outgrowth through interaction with multiple WAVE1 ligands. In fact, Strasser et al. have previously reported that the Arp2/3 complex is enriched in the central region of the growth cone but not in the peripheral region of the growth cone (51). We found that Sra-1 and WAVE1 were localized not only in the central region but also in the peripheral region of the growth cone.

CRMP-2 regulates axon formation via the Sra-1/WAVE1 complex. How does CRMP-2 regulate axon formation through Sra-1 and WAVE1? Here we found that the knockdown of CRMP-2, Sra-1, and WAVE1 or the expression of WAVE1 DN suppressed axon outgrowth and formation (Fig. 4 and 5). These results indicate that CRMP-2, Sra-1, and WAVE1 are required for axon outgrowth and formation. CRMP-2 D71N, which decreases the Sra-1-binding activity, lowers the axon outgrowth and multiple axons promoting activities compared to CRMP-2 WT (Fig. 4 and 5). The expression of the CRMP-2-binding region of Sra-1 801-1253 and WAVE1 DN or the knockdown of Sra-1 and WAVE1 inhibited the CRMP-2-induced axon outgrowth and multiple-axon formation (Fig. 4 and 5). Thus, CRMP-2 appears to induce axon outgrowth and formation via the Sra-1/WAVE1 complex.

CRMP-2 transports the Sra-1/WAVE1 complex to the growth cones of axons in a kinesin-1-dependent manner. Kinesin-1 (KIF5) preferentially accumulates in the initial segment of axons (40). The antibody inhibition of kinesin-1 blocks both plus- and minus-end-directed movement of axonal transport. Moreover, the treatment of the neurons with the antisense oligonucleotide for kinesin-1 decreases axon outgrowth and the transport of some proteins (15), which indicates that kinesin-1 is engaged in the transport of specific proteins to the growth cones of axons.

We have recently found that CRMP-2 directly binds to KLC and that kinesin-1 participates in the polarized distribution of CRMP-2 at the distal part of developing axons (30). In the present study, we found that CRMP-2 linked KLC to the Sra-1/WAVE1 complex (Fig. 6). The expression of CRMP-2 D71N and ΔN440 or the knockdown of CRMP-2 caused the delocalization of Sra-1 and WAVE1 from the growth cones of axons (Fig. 7). The knockdown of KLCs or the expression of KIF5A HL, which is a dominant-negative form of kinesin-1, induced the delocalization of CRMP-2, Sra-1, and WAVE1 (Fig. 8). Therefore, it seems that CRMP-2 enhances axon outgrowth and formation by transporting the Sra-1/WAVE1 complex to the growth cones of axons in a kinesin-1-dependent manner.

We speculate that CRMP-2 can regulate the activity of the Sra-1/WAVE1 complex in addition to the kinesin-1-dependent transport, because CRMP-2 interacts with tubulin heterodimers and promotes microtubule assembly (16). To examine the effects of CRMP-2 on Sra-1 and WAVE1, we expressed CRMP-2 WT and D71N in Vero fibroblasts and monitored actin cytoskeleton. So far, we did not observe the apparent effects of expression of CRMP-2 WT and D71N on actin cytoskeleton (data not shown). Eden et al. have previously reported that the addition of the GTP-bound form of Rac1, which is an active form, causes the dissociation of the Sra-2/WAVE1 complex, which releases active WAVE1 and leads to actin nucleation (14). We examined whether WAVE1 is dissociated from Sra-1 by the expression of CRMP-2 WT in HEK293 cells, which have the Sra-1/WAVE1 complex (Fig. S4). The dissociation of the Sra-1/WAVE1 complex by CRMP-2 WT was not observed under our conditions (data not shown). Further studies are necessary for elucidating the role of CRMP-2 in the regulation of Sra-1 and WAVE1 activities.

CRMP-2 acts as a cargo receptor for kinesin-1. The KLC C-terminal domain that consists of TPR motifs could be part of a protein interaction interface with a target molecule, such as amyloid precursor protein and c-jun NH2-terminal kinase (JNK)-interacting protein (JIP/SYD), on vesicular or organellar cargoes (3, 28, 57). Verhey et al. have previously found that the interaction between JIP-1 and KLC is necessary for JIP-1 to accumulate at the tip of neurites (57). JIP-1 interacts with dual leucine zipper-bearing kinase and ApoER2, which are neuron-specific upstream kinases of JNK and the receptor for the Reelin ligand, respectively. JIP-1 associates with the various signaling molecules and appears to act as a cargo receptor for kinesin-1 (55). These interactions may be necessary and important for neuronal development. CRMP-2 can link KLC to its interacting proteins, which are required for axon formation (16, 30, 41). Thus, CRMP-2 might serve as a cargo receptor for kinesin-1 and have an action similar to that of JIP-1. CRMP-2 seems to efficiently carry its interacting molecules such as the Sra-1/WAVE1 complex and tubulin heterodimer to the growth cones of developing axons in a kinesin-1-dependent manner. This transport system appears to enhance the reorganization of actin cytoskeleton and microtubule assembly in the growth cones of the future axons, thereby inducing axon outgrowth and formation.

ACKNOWLEDGMENTS

We thank Y. Ihara (University of Tokyo, Japan) and H. Okano (Keio University, Tokyo, Japan) for the kind gift of materials; M. Fukata, Y. Fukata, N. Arimura, T. Nishimura (Nagoya University, Aichi, Japan), N. Inagaki (NAIST, Nara, Japan), A. Hattori, K. Yamada, and A. Ogura (Nagoya University, Aichi, Japan) for helpful discussion and technical assistance; Y. Ito (Nagoya University, Aichi, Japan) for three-dimensional structure analysis; and T. Ishii for secretarial assistance.

This research was supported in part by Grants-in-Aid for Scientific Research from the Ministry of Education, Culture, Sports, Science and Technology of Japan (MEXT); Grant-in-Aid for Creative Scientific Research and The 21st Century Centre of Excellence (COE) Program from MEXT; Special Coordination Funds for Promoting Science and Technology (SCFPST); and the Organization for Pharmaceutical Safety and Research.

REFERENCES

1. **Arimura, N., N. Inagaki, K. Chihara, C. Menager, N. Nakamura, M. Amano, A. Iwamatsu, Y. Goshima, and K. Kaibuchi.** 2000. Phosphorylation of collapsin response mediator protein-2 by Rho-kinase. Evidence for two separate signaling pathways for growth cone collapse. J. Biol. Chem. **275:**23973–23980.
2. **Baas, P. W.** 1997. Microtubules and axonal growth. Curr. Opin. Cell Biol. **9:**29–36.

3. **Blatch, G. L., and M. Lassle.** 1999. The tetratricopeptide repeat: a structural motif mediating protein-protein interactions. Bioessays **21:**932–939.
4. **Bradke, F., and C. G. Dotti.** 2000. Establishment of neuronal polarity: lessons from cultured hippocampal neurons. Curr. Opin. Neurobiol. **10:**574–581.
5. **Bradke, F., and C. G. Dotti.** 1999. The role of local actin instability in axon formation. Science **283:**1931–1934.
6. **Brady, S. T.** 1985. A novel brain ATPase with properties expected for the fast axonal transport motor. Nature **317:**73–75.
7. **Brendza, K. M., D. J. Rose, S. P. Gilbert, and W. M. Saxton.** 1999. Lethal kinesin mutations reveal amino acids important for ATPase activation and structural coupling. J. Biol. Chem. **274:**31506–31514.
8. **Brown, M., T. Jacobs, B. Eickholt, G. Ferrari, M. Teo, C. Monfries, R. Z. Qi, T. Leung, L. Lim, and C. Hall.** 2004. α2-Chimaerin, cyclin-dependent kinase 5/p35, and its target collapsin response mediator protein-2 are essential components in semaphorin 3A-induced growth-cone collapse. J. Neurosci. **24:**8994–9004.
9. **Byk, T., S. Ozon, and A. Sobel.** 1998. The Ulip family phosphoproteins–common and specific properties. Eur. J. Biochem. **254:**14–24.
10. **Chalfie, M., E. Dean, E. Reilly, K. Buck, and J. N. Thomson.** 1986. Mutations affecting microtubule structure in Caenorhabditis elegans. J. Cell Sci. Suppl. **5:**257–271.
11. **Craig, A. M., and G. Banker.** 1994. Neuronal polarity. Annu. Rev. Neurosci. **17:**267–310.
12. **Deo, R. C., E. F. Schmidt, A. Elhabazi, H. Togashi, S. K. Burley, and S. M. Strittmatter.** 2004. Structural bases for CRMP function in plexin-dependent semaphorin3A signaling. EMBO J. **23:**9–22.
13. **Desai, C., G. Garriga, S. L. McIntire, and H. R. Horvitz.** 1988. A genetic pathway for the development of the Caenorhabditis elegans HSN motor neurons. Nature **336:**638–646.
14. **Eden, S., R. Rohatgi, A. V. Podtelejnikov, M. Mann, and M. W. Kirschner.** 2002. Mechanism of regulation of WAVE1-induced actin nucleation by Rac1 and Nck. Nature **418:**790–793.
15. **Ferreira, A., J. Niclas, R. D. Vale, G. Banker, and K. S. Kosik.** 1992. Suppression of kinesin expression in cultured hippocampal neurons using antisense oligonucleotides. J. Cell Biol. **117:**595–606.
16. **Fukata, Y., T. J. Itoh, T. Kimura, C. Menager, T. Nishimura, T. Shiromizu, H. Watanabe, N. Inagaki, A. Iwamatsu, H. Hotani, and K. Kaibuchi.** 2002. CRMP-2 binds to tubulin heterodimers to promote microtubule assembly. Nat. Cell Biol. **4:**583–591.
17. **Gaetano, C., T. Matsuo, and C. J. Thiele.** 1997. Identification and characterization of a retinoic acid-regulated human homologue of the unc-33-like phosphoprotein gene (hUlip) from neuroblastoma cells. J. Biol. Chem. **272:**12195–12201.
18. **Goshima, Y., F. Nakamura, P. Strittmatter, and S. M. Strittmatter.** 1995. Collapsin-induced growth cone collapse mediated by an intracellular protein related to UNC-33. Nature **376:**509–514.
19. **Govek, E. E., S. E. Newey, and L. Van Aelst.** 2005. The role of the Rho GTPases in neuronal development. Genes Dev. **19:**1–49.
20. **Gu, Y., N. Hamajima, and Y. Ihara.** 2000. Neurofibrillary tangle-associated collapsin response mediator protein-2 (CRMP-2) is highly phosphorylated on Thr-509, Ser-518, and Ser-522. Biochemistry **39:**4267–4275.
21. **Hedgecock, E. M., J. G. Culotti, J. N. Thomson, and L. A. Perkins.** 1985. Axonal guidance mutants of Caenorhabditis elegans identified by filling sensory neurons with fluorescein dyes. Dev. Biol. **111:**158–170.
22. **Hirokawa, N., and R. Takemura.** 2004. Kinesin superfamily proteins and their various functions and dynamics. Exp. Cell Res. **301:**50–59.
23. **Inagaki, N., K. Chihara, N. Arimura, C. Menager, Y. Kawano, N. Matsuo, T. Nishimura, M. Amano, and K. Kaibuchi.** 2001. CRMP-2 induces axons in cultured hippocampal neurons. Nat. Neurosci. **4:**781–782.
24. **Inatome, R., T. Tsujimura, T. Hitomi, N. Mitsui, P. Hermann, S. Kuroda, H. Yamamura, and S. Yanagi.** 2000. Identification of CRAM, a novel unc-33 gene family protein that associates with CRMP3 and protein-tyrosine kinase(s) in the developing rat brain. J. Biol. Chem. **275:**27291–27302.
25. **Innocenti, M., A. Zucconi, A. Disanza, E. Frittoli, L. B. Areces, A. Steffen, T. E. Stradal, P. P. Di Fiore, M. F. Carlier, and G. Scita.** 2004. Abi1 is essential for the formation and activation of a WAVE2 signalling complex. Nat. Cell Biol. **6:**319–327.
26. **Johnson, C. S., D. Buster, and J. M. Scholey.** 1990. Light chains of sea urchin kinesin identified by immunoadsorption. Cell Motil. Cytoskeleton **16:**204–213.
27. **Kamal, A., and L. S. Goldstein.** 2002. Principles of cargo attachment to cytoplasmic motor proteins. Curr. Opin. Cell Biol. **14:**63–68.
28. **Kamal, A., G. B. Stokin, Z. Yang, C. H. Xia, and L. S. Goldstein.** 2000. Axonal transport of amyloid precursor protein is mediated by direct binding to the kinesin light chain subunit of kinesin-I. Neuron **28:**449–459.
29. **Kawano, Y., Y. Fukata, N. Oshiro, M. Amano, T. Nakamura, M. Ito, F. Matsumura, M. Inagaki, and K. Kaibuchi.** 1999. Phosphorylation of myosin-binding subunit (MBS) of myosin phosphatase by Rho-kinase in vivo. J. Cell Biol. **147:**1023–1038.
30. **Kimura, T., N. Arimura, Y. Fukata, H. Watanabe, A. Iwamatsu, and K. Kaibuchi.** 2005. Tubulin and CRMP-2 complex is transported via Kinesin-1. J. Neurochem. **93:**1371–1382.
31. **Kobayashi, K., S. Kuroda, M. Fukata, T. Nakamura, T. Nagase, N. Nomura, Y. Matsuura, N. Yoshida-Kubomura, A. Iwamatsu, and K. Kaibuchi.** 1998. p140Sra-1 (specifically Rac1-associated protein) is a novel specific target for Rac1 small GTPase. J. Biol. Chem. **273:**291–295.
32. **Lawrence, C. J., R. K. Dawe, K. R. Christie, D. W. Cleveland, S. C. Dawson, S. A. Endow, L. S. Goldstein, H. V. Goodson, N. Hirokawa, J. Howard, R. L. Malmberg, J. R. McIntosh, H. Miki, T. J. Mitchison, Y. Okada, A. S. Reddy, W. M. Saxton, M. Schliwa, J. M. Scholey, R. D. Vale, C. E. Walczak, and L. Wordeman.** 2004. A standardized kinesin nomenclature. J. Cell Biol. **167:**19–22.
33. **Lee, S., J. H. Kim, C. S. Lee, Y. Kim, K. Heo, Y. Ihara, Y. Goshima, P. G. Suh, and S. H. Ryu.** 2002. Collapsin response mediator protein-2 inhibits neuronal phospholipase D(2) activity by direct interaction. J. Biol. Chem. **277:**6542–6549.
34. **Li, W.** 1992. Characterization of the *Caenorhabditis elegans* axonal guidance and outgrowth gene *unc-33* and a viariant Tc4 transposon. Ph.D. dissertation at University of Minnesota.
35. **Luo, L., Y. J. Liao, L. Y. Jan, and Y. N. Jan.** 1994. Distinct morphogenetic functions of similar small GTPases: Drosophila Drac1 is involved in axonal outgrowth and myoblast fusion. Genes Dev. **8:**1787–1802.
36. **Matsuura, Y., R. D. Possee, H. A. Overton, and D. H. Bishop.** 1987. Baculovirus expression vectors: the requirements for high level expression of proteins, including glycoproteins. J Gen. Virol. **68**(Part 5)**:**1233–1250.
37. **McIntire, S. L., G. Garriga, J. White, D. Jacobson, and H. R. Horvitz.** 1992. Genes necessary for directed axonal elongation or fasciculation in C. elegans. Neuron **8:**307–322.
38. **Miki, H., S. Suetsugu, and T. Takenawa.** 1998. WAVE, a novel WASP-family protein involved in actin reorganization induced by Rac. EMBO J. **17:**6932–6941.
39. **Minturn, J. E., H. J. Fryer, D. H. Geschwind, and S. Hockfield.** 1995. TOAD-64, a gene expressed early in neuronal differentiation in the rat, is related to unc-33, a C. elegans gene involved in axon outgrowth. J. Neurosci. **15:**6757–6766.
40. **Nakata, T., and N. Hirokawa.** 2003. Microtubules provide directional cues for polarized axonal transport through interaction with kinesin motor head. J. Cell Biol. **162:**1045–1055.
41. **Nishimura, T., Y. Fukata, K. Kato, T. Yamaguchi, Y. Matsuura, H. Kamiguchi, and K. Kaibuchi.** 2003. CRMP-2 regulates polarized Numb-mediated endocytosis for axon growth. Nat. Cell Biol. **5:**819–826.
42. **Nishimura, T., K. Kato, T. Yamaguchi, Y. Fukata, S. Ohno, and K. Kaibuchi.** 2004. Role of the PAR-3-KIF3 complex in the establishment of neuronal polarity. Nat. Cell Biol. **6:**328–334.
43. **Nishimura, T., T. Yamaguchi, K. Kato, M. Yoshizawa, Y. Nabeshima, S. Ohno, M. Hoshino, and K. Kaibuchi.** 2005. PAR-6-PAR-3 mediates Cdc42 signaling to Rac activation through STEF/Tiam1, RacGEFs. Nat. Cell Biol. **7:**270–277.
44. **Noda, Y., Y. Okada, N. Saito, M. Setou, Y. Xu, Z. Zhang, and N. Hirokawa.** 2001. KIFC3, a microtubule minus end-directed motor for the apical transport of annexin XIIIb-associated triton-insoluble membranes. J. Cell Biol. **155:**77–88.
45. **Schenck, A., B. Bardoni, C. Langmann, N. Harden, J. L. Mandel, and A. Giangrande.** 2003. CYFIP/Sra-1 controls neuronal connectivity in Drosophila and links the Rac1 GTPase pathway to the fragile X protein. Neuron **38:**887–898.
46. **Schenck, A., B. Bardoni, A. Moro, C. Bagni, and J. L. Mandel.** 2001. A highly conserved protein family interacting with the fragile X mental retardation protein (FMRP) and displaying selective interactions with FMRP-related proteins FXR1P and FXR2P. Proc. Natl. Acad. Sci. USA **98:**8844–8849.
47. **Shi, S. H., L. Y. Jan, and Y. N. Jan.** 2003. Hippocampal neuronal polarity specified by spatially localized mPar3/mPar6 and PI 3-kinase activity. Cell **112:**63–75.
48. **Soderling, S. H., K. L. Binns, G. A. Wayman, S. M. Davee, S. H. Ong, T. Pawson, and J. D. Scott.** 2002. The WRP component of the WAVE-1 complex attenuates Rac-mediated signalling. Nat. Cell Biol. **4:**970–975.
49. **Steffen, A., K. Rottner, J. Ehinger, M. Innocenti, G. Scita, J. Wehland, and T. E. Stradal.** 2004. Sra-1 and Nap1 link Rac to actin assembly driving lamellipodia formation. EMBO J. **23:**749–759.
50. **Stradal, T. E., K. Rottner, A. Disanza, S. Confalonieri, M. Innocenti, and G. Scita.** 2004. Regulation of actin dynamics by WASP and WAVE family proteins. Trends Cell Biol. **14:**303–311.
51. **Strasser, G. A., N. A. Rahim, K. E. VanderWaal, F. B. Gertler, and L. M. Lanier.** 2004. Arp2/Arp3 is a negative regulator of growth cone translocation. Neuron **43:**81–94.
52. **Suetsugu, S., H. Miki, and T. Takenawa.** 1999. Identification of two human WAVE/SCAR homologues as general actin regulatory molecules which associate with the Arp2/3 complex. Biochem. Biophys. Res. Commun. **260:**296–302.
53. **Takenawa, T., and H. Miki.** 2001. WASP and WAVE family proteins: key molecules for rapid rearrangement of cortical actin filaments and cell movement. J. Cell Sci. **114:**1801–1809.

54. **Terada, S., M. Kinjo, and N. Hirokawa.** 2000. Oligomeric tubulin in large transporting complex is transported via kinesin in squid giant axons. Cell **103:**141–155.
54a. **Tsuboi, D., T. Hikita, H. Qadota, M. Amano, and K. Kaibuchi.** J. Neurochem., in press.
55. **Vale, R. D.** 2003. The molecular motor toolbox for intracellular transport. Cell **112:**467–480.
56. **Vale, R. D., T. S. Reese, and M. P. Sheetz.** 1985. Identification of a novel force-generating protein, kinesin, involved in microtubule-based motility. Cell **42:**39–50.
57. **Verhey, K. J., D. Meyer, R. Deehan, J. Blenis, B. J. Schnapp, T. A. Rapoport, and B. Margolis.** 2001. Cargo of kinesin identified as JIP scaffolding proteins and associated signaling molecules. J. Cell Biol. **152:**959–970.
58. **Wang, L. H., and S. M. Strittmatter.** 1997. Brain CRMP forms heterotetramers similar to liver dihydropyrimidinase. J. Neurochem. **69:**2261–2269.
59. **Westphal, R. S., S. H. Soderling, N. M. Alto, L. K. Langeberg, and J. D. Scott.** 2000. Scar/WAVE-1, a Wiskott-Aldrich syndrome protein, assembles an actin-associated multi-kinase scaffold. EMBO J. **19:**4589–4600.
60. **Yoshimura, T., Y. Kawano, N. Arimura, S. Kawabata, A. Kikuchi, and K. Kaibuchi.** 2005. GSK-3β regulates phosphorylation of CRMP-2 and neuronal polarity. Cell **120:**137–149.
61. **Zallen, J. A., Y. Cohen, A. M. Hudson, L. Cooley, E. Wieschaus, and E. D. Schejter.** 2002. SCAR is a primary regulator of Arp2/Arp3-dependent morphological events in Drosophila. J. Cell Biol. **156:**689–701.